

The origin of enhanced optical absorption in solar cells with metal nanoparticles embedded in the active layer

Jung-Yong Lee and Peter Peumans*

Department of Electrical Engineering, Stanford University, 330 Serra Mall, Stanford, CA 94305

*ppeumans@stanford.edu

Abstract: We analyze the enhancement in optical absorption of an absorbing medium when spherical metal nanoparticles are embedded in it. Our analysis uses generalized Mie theory to calculate the absorbed optical power as a function of the distance from the metal nanoparticle. This analysis is used to evaluate the potential of enhancing optical absorption in thin-film solar cells by embedding spherical metal nanoparticles. We consider the trade-off between maximizing overall optical absorption and ensuring that a large fraction of the incident optical power is dissipated in the absorbing host medium rather than in the metal nanoparticle. We show that enhanced optical absorption results from strong scattering by the metal nanoparticle which locally enhances the optical electric fields. We also discuss the effect of a thin dielectric encapsulation of the metal nanoparticles.

©2010 Optical Society of America

OCIS codes: (250.5403) Plasmonics; (290.4020) Mie theory.

References and links

1. D. M. Schaadt, B. Feng, and E. T. Yu, "Enhanced semiconductor optical absorption via surface plasmon excitation in metal nanoparticles," *Appl. Phys. Lett.* **86**(6), 063106 (2005).
2. S. Pillai, K. R. Catchpole, T. Trupke, and M. A. Green, "Surface plasmon enhanced silicon solar cells," *J. Appl. Phys.* **101**(9), 093105–093108 (2007).
3. H. R. Stuart, and D. G. Hall, "Absorption enhancement in silicon-on-insulator waveguides using metal island films," *Appl. Phys. Lett.* **69**(16), 2327–2329 (1996).
4. B. P. Rand, P. Peumans, and S. R. Forrest, "Long-range absorption enhancement in organic tandem thin-film solar cells containing silver nanoclusters," *J. Appl. Phys.* **96**(12), 7519–7526 (2004).
5. K. R. Catchpole, and A. Polman, "Design principles for particle plasmon enhanced solar cells," *Appl. Phys. Lett.* **93**(19), 191113 (2008).
6. S. Pillai, K. R. Catchpole, T. Trupke, G. Zhang, J. Zhao, and M. A. Green, "Enhanced emission from Si-based light-emitting diodes using surface plasmons," *Appl. Phys. Lett.* **88**(16), 161102–161103 (2006).
7. S. Fujimori, R. Dinyari, J.-Y. Lee, and P. Peumans, "Plasmonic light concentration in organic solar cells," accepted in *Nano Lett.* (2009).
8. A. Luque, and S. Hegedus, eds., *Handbook of Photovoltaic Science and Engineering* (John Wiley & Sons, Ltd, 2003).
9. P. Peumans, V. Bulovic, and S. R. Forrest, "Efficient photon harvesting at high optical intensities in ultrathin organic double-heterostructure photovoltaic diodes," *Appl. Phys. Lett.* **76**(19), 2650–2652 (2000).
10. E. Yablonovitch, and G. D. Cody, "Intensity enhancement in textured optical sheets for solar cells," *IEEE Trans. Electron. Dev.* **29**(2), 300–305 (1982).
11. J. Müller, B. Rech, J. Springer, and M. Vanecek, "TCO and light trapping in silicon thin film solar cells," *Sol. Energy* **77**(6), 917–930 (2004).
12. C. F. Bohren, and D. R. Huffman, *Absorption and Scattering of Light by Small Particles* (Wiley, New York, 1983).
13. G. Mie, "Beiträge zur Optik trüber Medien, speziell kolloidaler Metallösungen," *Annalen der Physik* **330**(3), 377–445 (1908).
14. Q. Fu, and W. Sun, "Mie theory for light scattering by a spherical particle in an absorbing medium," *Appl. Opt.* **40**(9), 1354–1361 (2001).
15. I. W. Sudiarta, and P. Chylek, "Mie-scattering formalism for spherical particles embedded in an absorbing medium," *J. Opt. Soc. Am. A* **18**(6), 1275–1278 (2001).

Metal nanostructures are drawing attention for use in optoelectronic devices such as photovoltaic (PV) cells [1–5] and light emitting devices (LEDs) [6] as a means to modify the strength of optical interactions. In the case of PV cells, it was shown that incorporating metal nanoparticles (MNPs) leads to locally enhanced optical absorption and an overall increase in the power conversion efficiency [4,7]. In general, the increased strength of the optical interactions with the host material due to the presence of metal nanostructures allows for the use of a thinner layer of active material, alleviating the trade-off between optical absorption and internal quantum efficiency(IQE) [8,9]. This in turn can result in improved overall power conversion efficiency. In some cases, the enhanced absorption is a *far-field* effect and is due to scattering of incident light into waveguided modes or modes trapped by total internal reflection [1–3,5] [see Fig. 1(a)]. In such case, the MNPs have the same function as a more conventional textured surface [10] that is typically used to increase the optical path length and decrease reflection losses in solar cells. MNPs are attractive in this case since they may be easier or cheaper to fabricate, or exhibit a higher performance compared to conventional dielectric light scattering approaches. These advantages are more important for thin-film devices since conventional texturing approaches are less effective for film thicknesses approaching the wavelength of light [11].

Here, we focus on the *near-field* enhancement in optical absorption due to the presence of MNPs or more complex metal nanostructures [2] [see Fig. 1(b)]. We provide an analytical analysis and physical interpretation of the origin of the enhancement of the optical absorption of a host material when spherical MNPs are embedded. The spherical geometry was chosen because of its simplicity which allows us to analytically identify the contributions to the enhanced optical absorption. Many reports have considered the scattering and extinction by a spherical particle in non-absorbing [12,13] and absorbing media [14,15], but few reports have quantitatively analyzed the increased optical absorption of an absorbing host in the near-field of a metal nanoparticle. This effect is sometimes referred to as a plasmonic enhancement. As shown below, this is inaccurate. The effects persist for perfect electrical conductors which support no plasmon modes. The enhanced optical absorption is better described as the result of strong scattering and concentration of the optical electric field near the MNPs.

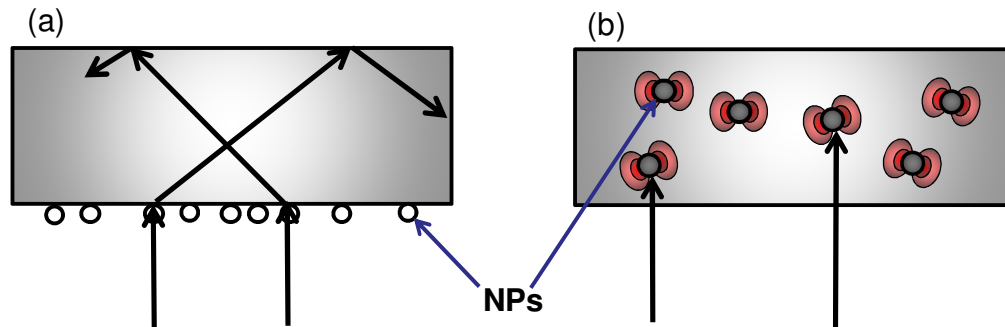


Fig. 1. (a) Schematic of a photovoltaic cell with MNPs placed on the surface of the cell. Enhancement of optical absorption is a *far-field* effect caused by the redirection of light into guided or trapped modes. (b) Schematic of a photovoltaic cell with MNPs embedded in the active layer. In this case, enhancement of optical absorption can result from *near-field* coupling which exploits the locally enhanced optical electric fields.

The classical Mie approach [13] formulates light scattering and absorption by a spherical particle embedded in a homogeneous non-absorbing medium. However, to evaluate the optical absorption of an absorbing host medium, a generalization is necessary. Previously reported generalized Mie approaches have focused on the spherical particle itself, and estimated optical absorption integrated over the volume of the MNP [14,15]. Here, we extend

the analysis to an arbitrary surface extending beyond the MNP surface to evaluate the optical absorption of the surrounding absorbing medium.

We consider an incident plane wave propagating in the positive z direction. E_i and H_i are defined as the incident electric and magnetic fields, respectively. The electric and magnetic fields scattered by the MNP are denoted as E_s and H_s , respectively. The absorbed power within an imaginary sphere of radius R , W_{abs} , can be written in terms of components due to the incident power, W_i , scattered power, W_s , and a cross-term, W_{ext} :

$$\begin{aligned} W_{abs}(R) &= -\frac{1}{2} \operatorname{Re} \oint_{r=R} [(E_i + E_s) \times (H_i^* + H_s^*)] \cdot ds \\ &= -\operatorname{Re} \oint_{r=R} \frac{1}{2} (E_i \times H_i^*) \cdot ds - \operatorname{Re} \oint_{r=R} \frac{1}{2} (E_s \times H_s^*) \cdot ds - \operatorname{Re} \oint_{r=R} \frac{1}{2} (E_i \times H_s^* + E_s \times H_i^*) \cdot ds \\ &= W_i - W_s + W_{ext} \end{aligned} \quad (1)$$

Note that the sign of W_s is chosen such that it is positive if power leaves the sphere of interest. These components of absorbed power can be expressed in terms of Riccati-Bessel functions [12]:

$$\psi_n(\rho) = \rho \cdot j_n(\rho), \quad \xi_n(\rho) = \rho \cdot h_n^{(1)}(\rho), \quad (2)$$

where $j_n(\rho)$ is a spherical Bessel function and $h_n^{(1)}(\rho)$ is a Hankel function. The terms of Eq. (1) are:

$$W_i(R) = \frac{\pi |E_0|^2}{\omega} \sum_n (2n+1) \operatorname{Im} \left(\frac{\psi_n \psi_n^* - \psi_n' \psi_n'^*}{k \mu^*} \right), \quad (3)$$

$$W_s(R) = \frac{\pi |E_0|^2}{\omega} \sum_n (2n+1) \operatorname{Im} \left(\frac{|a_n|^2 \xi_n' \xi_n'^* - |b_n|^2 \xi_n \xi_n^*}{k \mu^*} \right), \quad (4)$$

$$W_{ext}(R) = \frac{\pi |E_0|^2}{\omega} \sum_n (2n+1) \operatorname{Im} \left(\frac{a_n^* \psi_n' \xi_n'^* - b_n^* \psi_n \xi_n^* + a_n \xi_n' \psi_n'^* - b_n \xi_n \psi_n^*}{k \mu^*} \right). \quad (5)$$

where we followed the notations of Ref [12]. and the functions ψ_n and ξ_n are evaluated at $\rho = R$. a_n and b_n are scattering coefficients, k is wavenumber, and μ is the permeability of host material. The total absorbed power can be written in compact form as:

$$W_{abs}(R) = \frac{\pi |E_0|^2}{\omega} \sum_n (2n+1) \operatorname{Im} \left(\frac{A_n}{k \mu^*} \right). \quad (6)$$

where

$$A_n = -(a_n \xi_n' - \psi_n')(a_n^* \xi_n'^* - \psi_n'^*) + (b_n \xi_n - \psi_n)(b_n^* \xi_n^* - \psi_n^*) \quad (7)$$

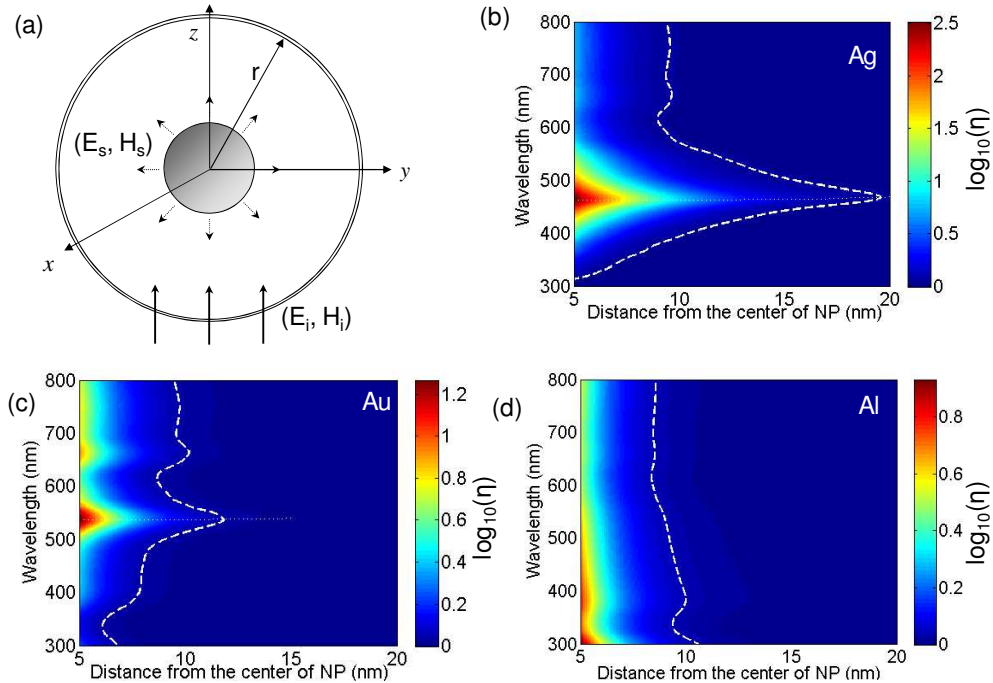


Fig. 2. (a) Schematic of a MNP embedded in a host material system. (b)-(d) Spectrally-resolved enhancement of absorbed optical power when a 10nm-diameter MNP is embedded integrated over the volume of a 0.1nm-thick shell concentric with the MNP as a function of shell radius. The colorscale is logarithmic. The calculation was performed for Ag (b), Au (c), and Al (d). The shell radius for at which the absorption is enhanced by 10% is indicated by a white dashed line

This modified Mie solution allows us to evaluate the spatial extent of the enhancement in optical absorption. Figure 2 shows the spectrally-resolved enhancement in the optical power absorbed in the absorbing medium, η , on a \log_{10} -scale. The enhancement is evaluated within a 0.1nm-thick shell in the presence of a 5nm-radius MNP over the case without a MNP (the metal is replaced by the absorbing medium):

$$\eta = \frac{[W_{abs}(r+0.1\text{nm}) - W_{abs}(r)]_{\text{with metal NP}}}{[W_{abs}(r+0.1\text{nm}) - W_{abs}(r)]_{\text{without metal NP}}}, \quad (8)$$

the upper bound of which can be approximated as $\eta = 1 + \left| 2 \left(\frac{a}{r} \right)^3 \frac{m_i^2 - m^2}{m_i^2 + 2m^2} \right|^2$.

We note that this enhancement is averaged over the volume of the shell. There may be stronger local enhancements, for example near the equator of the MNP [see below and Fig. 3(b)]. For the absorbing material, the optical properties of copper phthalocyanine (CuPc, a typical absorber used in organic solar cells) were used, while the optical properties of Ag, Au, and Al were used for the MNP [Figs. 2(b), 2(c), and 2(d), respectively]. The enhancement in optical absorption is strongest for Ag and coincides with the plasmon resonance of a spherical Ag particle at $\lambda = 460$ nm. The enhancement drops quickly as a function of distance away from the MNP surface. For example, for a Ag sphere at $\lambda = 460$ nm, the enhancement drops below 10% at a radius of $r = 18.8$ nm. For Au at $\lambda = 540$ nm, this radius is 11.8 nm, and for Al at 400nm, it is 9.9 nm. For a perfect metal (approximated by a refractive index of $1 + 10^4i$), this radius is 8.3 nm, and the enhancement never exceeds 3 even when the shell is

located very close to the MNP surface because we are considering averages over a whole shell. We also note that, for all three metals considered, the enhancement in optical absorption extends to longer wavelengths away from the plasmon resonance and within a sphere with approximately 10 nm of radius. The nature of this absorption enhancement is further elucidated below.

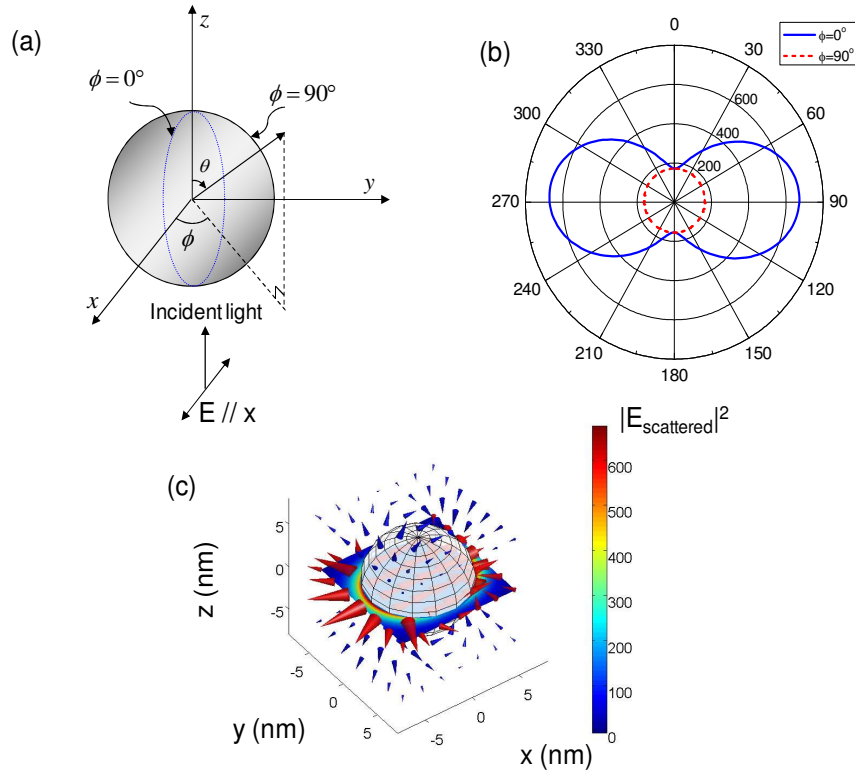


Fig. 3. (a) Schematic showing the direction and polarization of incident light and where scattered fields are calculated. (b) $|E_{scattered}|^2$ as a function of polar angle (θ) for both $\varphi = 0^\circ$ (blue solid line) and $\varphi = 90^\circ$ (red dotted line) for $\lambda = 460$ nm. (c) $\text{Re}(E_{total})$ at $z = -6$ nm (blue cones), 0 (red cones), and 6 nm (blue cones) planes for $\lambda = 460$ nm. $|E_{total}|^2$ is also plotted in the $z = 0$ nm plane as a colormap.

Figure 3(b) shows the intensity of the scattered electric field, $|E_s|^2$, normalized to the intensity of the incident field, $|E_i|^2$, as a function of polar angle, θ , when the azimuthal angle φ is 0° (aligned with incident light polarization) and 90° [see Fig. 3(a) for a definition of φ and θ], respectively, for a 10 nm-diameter Ag MNP at plasmon resonance conditions ($\lambda = 460$ nm). At the equator of the MNP and for $\varphi = 0^\circ$, $|E_s|^2$ is 670 times larger than the incident optical electric field intensity, $|E_i|^2$. Even at 90° off the incident electric field (for $\varphi = 90^\circ$), $|E_s|^2$ is 155 times larger than the incident optical electric field intensity, $|E_i|^2$. Figure 3(c) shows $\text{Re}[E_i + E_s]$ for $\lambda = 460$ nm in the immediate vicinity of the Ag MNP in

which the vector field is represented as cones whose size is proportional to field magnitude. $|E_i + E_s|^2$ on $z = 0$ plane is also shown in the same plot.

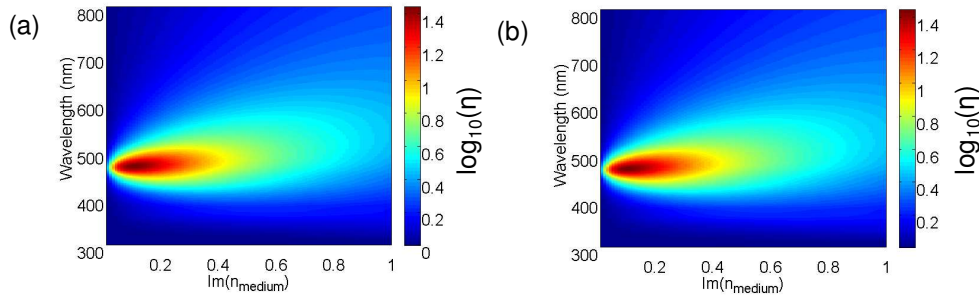


Fig. 4. Enhancement in optical absorption efficiency in the region bound by $r = 5$ nm and $r = 10$ nm when a 10 nm-diameter Ag MNP is embedded as a function of imaginary part of refractive index of medium (real part is set as 1.8). (b) Difference of the scattered power entering the same region as in (a) at $r = 5$ nm and exiting at $r = 10$ nm. The similarity with (a) indicates that the increased in optical absorption comes mostly from re-absorption by scattering.

Figure 4(a) shows the *increase* in absorption efficiency within a 5 nm-thick shell (extending from a 5 nm to 10 nm radius) compared to the case without Ag MNP (i.e. the space occupied by the Ag MNP is filled with the host material) as a function of the imaginary component k of the refractive index $n + ik$ (n is held constant at 1.8, typical for an organic absorber) and wavelength. The increase in optical absorption extends over a broad spectral range, especially for a strong absorber ($k > 0.5$). This increase in optical absorption results primarily from the absorption of light scattered by the MNPs. This is shown in Fig. 4 by comparing the increased in optical absorption efficiency in a 5 nm-thick shell around the metal nanoparticle [Fig. 4(a)] with the difference of the scattered power entering this shell at $r = 5$ nm and exiting the shell at $r = 10$ nm [Fig. 4(b)]. Since these two plots are nearly identical, the increased optical absorption is entirely due to the scattered power term, $W_s(R)$, with the cross-term, $W_{ext}(R)$, playing a minor role.

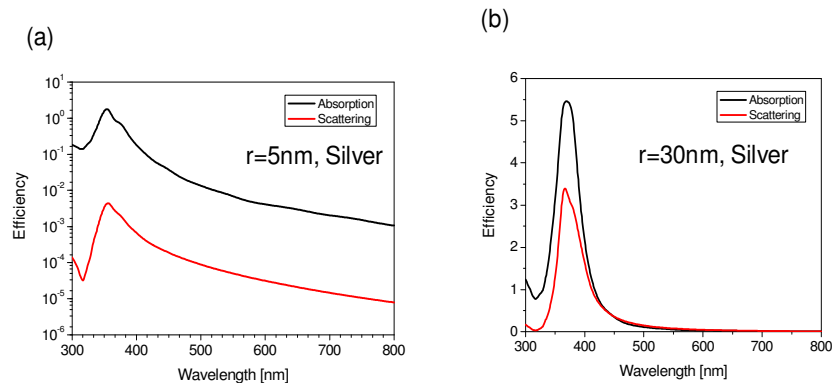


Fig. 5. (a) Absorption and scattering efficiency for a 10 nm-diameter Ag MNP in vacuum. (b) Absorption and scattering efficiency of 30 nm-diameter Ag MNP in vacuum.

For a 5 nm-radius Ag MNP in vacuum, the scattered power is orders of magnitude lower than the power absorbed by the nanoparticle as shown in Fig. 5(a). In order for the scattered power to be comparable to the absorbed power, the radius of the metal nanoparticle has to be much larger, e.g. 30 nm [Fig. 5(b)]. This appears to lead to the conclusion that larger MNPs

are required to effectively enhance optical absorption of a medium without causing undue absorption by the metal nanoparticle itself. However, as shown here, when the nanoparticle is surrounded by an absorbing medium, the scattered power becomes comparable to the power absorbed by the MNP, leading to enhanced optical absorption in the surrounding absorbing medium. It will be shown below that this enhancement in optical absorption of the host material can be obtained without significant optical absorption by the metal nanosphere itself. Another important conclusion from Fig. 4 is that maximal enhancement of optical absorption of the host material occurs for relatively low values of the imaginary part of the index of refraction ($k = 0.1$, $\lambda = 460$ nm). This can be explained as follows. Assuming $|m_t/m|ka < 1$, which is mostly true when particle's size is much smaller than wavelengths, the scattered optical electric field, E_s , can be approximated as:

$$E_s = \sum_{n=1}^{\infty} E_0 i^n \frac{2n+1}{n(n+1)} (i a_n N_{e1n}^{(3)} - b_n M_{o1n}^{(3)}) \cong -\frac{3}{2} E_0 a_1 N_{e1n}^{(3)}, \quad (9)$$

since all coefficients a_n and b_n other than a_1 are negligible compared to a_1 . where,

$$a_1 \cong -\frac{i2(mka)^3}{3} \frac{m_t^2 - m^2}{m_t^2 + 2m^2}, \quad (10)$$

and since

$$|N_{e1n}^{(3)}| \propto \frac{1}{|mkr|^3} \quad (11)$$

the power absorbed by scattering from the infinitesimal volume dv is,

$$w_s = \frac{1}{2} \omega \varepsilon'' |E_s|^2 dv \propto \frac{\text{Re}(m) \cdot \text{Im}(m)}{\lambda} \left| \frac{m_t^2 - m^2}{m_t^2 + 2m^2} \right|^2 dv \quad (12)$$

At $\lambda = 460$ nm, w_s is maximal for $k = 0.1$, which coincides with the rigorous analysis.

Note that the polarizability of the nanosphere is proportional to $\frac{m_t^2 - m^2}{m_t^2 + 2m^2}$, which determines

the strength of absorption of the nanosphere. In case of a Ag nanosphere, this factor decreases as k increases. Strong re-absorption by scattering results from a competition between absorption due to the bulk properties ($\text{Im}(m)$) and enhanced optical fields $\left(\left| \frac{m_t^2 - m^2}{m_t^2 + 2m^2} \right| \right)$. This

is analogous to a lossy cavity with lossy mirrors. For relatively loss-free (i.e. transparent) media, optical absorption in the metal nanoparticle (equivalent of the cavity mirrors) dominates, while for lossier media, the optical absorption mostly takes place in the absorber, but the enhancement in absorption becomes limited because the cavity quality factor reduces.

For use in the active layer of a solar cell, the relevant parameter that needs to be optimized is the increase in optical absorption in the absorber compared to the case where the metal nanosphere is replaced by the absorber material. At the same time, the fraction of power absorbed in the metal nanosphere must be minimized. As a measure of the efficiency of light scattering, i.e. the benefits of the MNP, Fig. 6 shows $W_s(a)/W_i(a)$ as a function of wavelength and imaginary number of host material's refractive index for a Ag NP and a host material with $n = 1.8$. The radius of the MNP is 5nm. Note that $W_s(a)$ represents the optical absorption obtained by virtue of the presence of the MNP as explained in Fig. 5, and $W_i(a)$ is

the optical power absorbed by the volume that the MNP replaces. Therefore, for $W_s(a)/W_i(a) > 1$, incorporating the MNPs should be considered since it results in an increased overall optical absorption. Although the enhancement is < 1 for $\lambda < 350\text{nm}$, the overall enhancement is typically > 3 for most absorbers and most of the solar spectrum. This is surprising for several reasons. First, small ($\sim 10\text{nm}$ diameter) MNPs can be used to enhance optical absorption in the host material. Second, the enhancement in optical absorption persists even for wavelengths longer than the plasmon resonance wavelength of the MNP.

Consider an absorbing material with a density, N (m^{-3}), of embedded 5 nm-radius Ag MNPs. The total intensity loss, dI , through infinitesimal layer, dz is

$$dI = -I\alpha_0 \left(1 - \frac{4}{3}\pi \cdot r^3 N \right) dz - I \cdot C_a N dz - I \cdot C_s N dz \quad (13)$$

where the first term is power absorption by bulk host material excluding the volumes occupied by the nanoparticles, the second term absorption by the nanoparticles themselves,

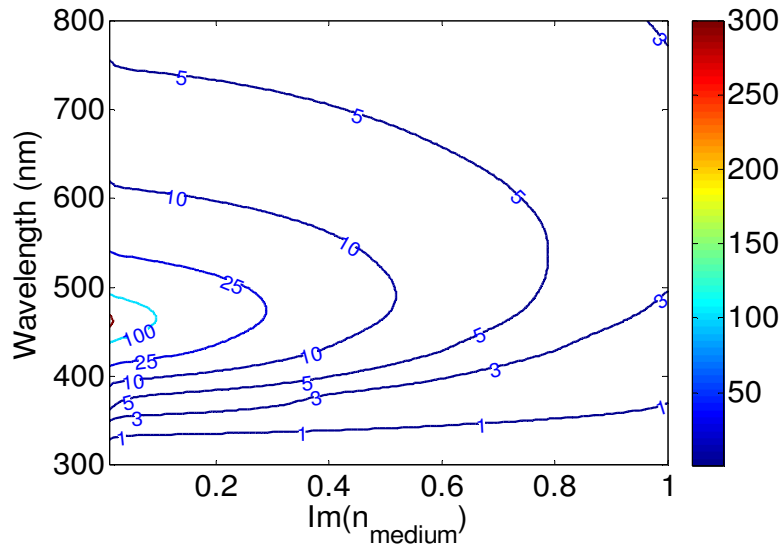


Fig. 6. Enhancement in optical absorption obtained by embedding Ag MNPs in the host medium. This enhancement is calculated as the ratio of optical power scattered by the MNPs over the optical that would be absorbed if the MNP were replaced by the host material.

and the third term scattered power by the nanoparticles, which will be re-absorbed power by the host material. C_a and C_s are absorption and scattering cross section, respectively, which are defined as the power divided by incident power.

The transmitted light intensity through film with thickness d will be then

$$I = I_0 \exp \left(-\alpha_0 \left(1 - \frac{4}{3}\pi \cdot r^3 N \right) - (C_a + C_s) N \right) d \quad (14)$$

The fraction $\left[\alpha_0 \left(1 - \frac{4}{3}\pi \cdot r^3 N \right) + C_s N \right] / \left[\alpha_0 \left(1 - \frac{4}{3}\pi \cdot r^3 N \right) + (C_a + C_s) N \right]$ of absorbed power is attributed to absorption in the host material. The optical absorption for a 10 nm-thick film with $N = 1/(15 \times 10^{-9})^3 \text{m}^{-3}$ is shown in Fig. 7(a). The host material absorbs more strongly when nanospheres are embedded (blue line) compared to the case of a homogeneous host material (black line). We note that the nanospheres absorb most of the incident power for

the spectral range where the host material's absorption coefficients are negligible (400 nm-500 nm). There is a significant enhancement in the optical absorption over a broad spectral range for $\lambda > 550$ nm without a penalty of a large fraction of the incident light being absorbed by the Ag nanospheres. This is consistent with a previously reported broadband absorption enhancement obtained when Ag nanospheres were embedded in an organic thin-film solar cell [4].

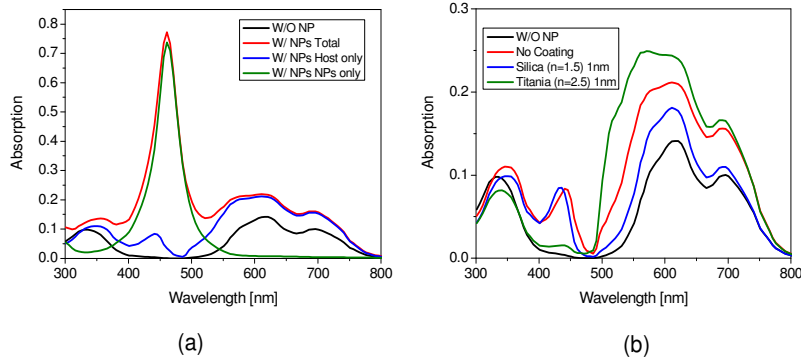


Fig. 7. (a) Absorption in Ag MNPs (green line) and CuPc host material (blue line) for a MNP concentration of $1/(15\text{nm})^3$ and 10 nm film thickness. The total absorption (red line) and absorption for the case of a homogeneous CuPc film (black line) are also shown. (b) Absorption of the CuPc host material when 10 nm-diameter Ag MNPs are embedded for bare MNPs (red line), 1nm-thick silica-coated ($n = 1.5$) MNPs (blue line), and 1nm-thick titania-coated ($n = 2.5$) MNPs (green line). The absorption of CuPc in the absence of MNPs is plotted for reference (black line).

The ability to enhance optical absorption locally on a nanometer-scale makes this approach particularly attractive for organic photovoltaic cells, where there is a mismatch between the optical absorption length (100-200 nm) and the exciton diffusion length (~ 10 nm). Embedding metal nanostructures near the active interface leads to concentrated optical electric fields near the junction [7] which results in more excitons being created within an exciton diffusion length away from the active interface. To evaluate the effect of the presence of metal NPs on the efficiency of a solar cell, the optical model must be combined with a charge carrier and/or exciton diffusion model, as was done in Ref [7]. We also note that, in practice, the metal nanospheres have to be separated from the semiconducting absorber by a thin dielectric to prevent exciton quenching through dipole-dipole interaction and charge trapping. Adding a 2-3nm thick dielectric coating (e.g. SiO_2 or TiO_2) would be sufficient to prevent adverse effects while offering an extra degree of tenability in spectral response and degree of enhancement of optical absorption. The plasmon resonance peak is red-shifted if the index of the dielectric coating is larger than that of the host material, or blue-shifted otherwise. If Ag nanospheres are encapsulated with a 1nm-thick TiO_2 coating [$n = 2.5$, green line, Fig. 7(b)], the plasmon resonance peak shifts to longer wavelengths and the optical absorption of the host material for $\lambda = 500$ -800 nm is increased over the case without a dielectric coating (red line). On the other hand, if the Ag nanospheres are encapsulated with a 1 nm-thick SiO_2 ($n = 1.5$, blue line) coating, the optical absorption decreases over the same spectral range.

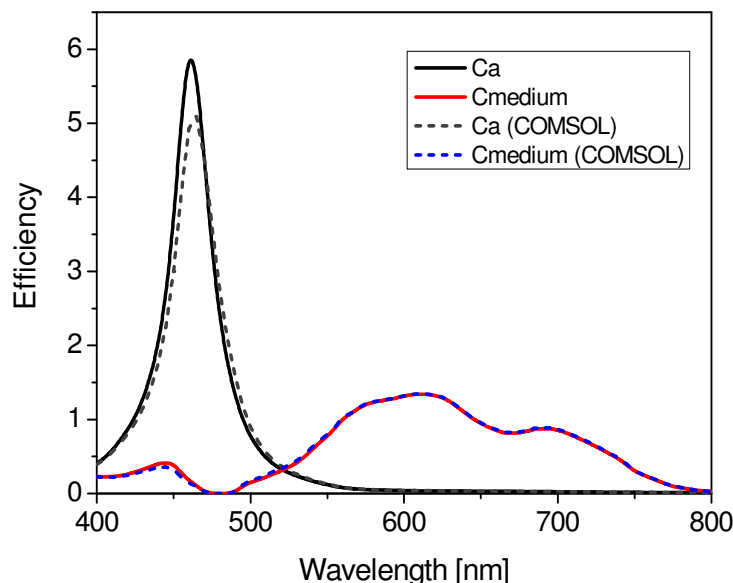


Fig. 8. Comparison between analytical calculations (solid lines) and optical simulations (dotted lines) of the optical absorption in the host material and MNPs for a system consisting of 10 nm-diameter Ag MNPs embedded in CuPc.

In Fig. 8, we compare the results of our analytical model with those obtained using optical modeling software that uses the finite-element method [16]. The optical absorption in the Ag nanosphere and the surrounding CuPc host material was calculated. A $50 \text{ nm} \times 50 \text{ nm} \times 50 \text{ nm}$ domain was used with a 10 nm-diameter Ag nanosphere placed at the center. A 10 nm-radius virtual sphere was used to measure the optical power absorbed in the Ag nanosphere and CuPc. The close match confirms that the analysis presented here provides an accurate and fast estimate of the enhancement in optical absorption. The analytical model is evaluated within 0.1 sec per wavelength on a desktop PC, while the optical modeling software requires >2000 sec for the same calculation.

In conclusion, a generalized Mie approach was used to understand the nature of and quantitatively analyze the optical absorption enhancement when a MNPs are embedded in an absorbing medium. This effect was observed in thin-film organic solar cells and increases device performance by increasing the optical absorption probability. This effect was confirmed in optical modeling, but no analytical analysis of the physical underpinnings of the effects has been reported. Our analysis reveals that the enhanced optical absorption is the result of strong scattering which leads to stronger local optical electric fields and therefore stronger localized optical absorption. The enhancement extends to wavelengths longer than the plasmon resonance wavelength for which the losses in the metallic particles become insignificant. Dielectric coatings on the MNPs can be used to tune its resonance wavelength.

Acknowledgements

This work was supported by the National Science Foundation and KAUST (King Abdullah University of Science and Technology). JYL would like to thank The Korea Foundation for Advanced Studies for its support.